



## Influence of synthetic wastewater on the transport and transformation in irrigated soils

A. Erfani Agah<sup>a,b,\*</sup>, P. Meire<sup>a</sup>, E. De Deckere<sup>a</sup>

<sup>a</sup>Department of Biology, University of Antwerp, Campus DrieEiken, D.C.115, Universiteitsplein 1, 2610 Wilrijk, Antwerp, Belgium, Tel. +32 3 265 2274, Fax +32 3 265 22 71, email: Ali.Erfaniagah@student.uantwerpen.be, Ali.Erfani68@gmail.com (A.E. Agah), patrick.meire@uantwerpen.be (P. Meire), eric.dedeckere@haven.antwerpen.be (E. De Deckere)

<sup>b</sup>Department of Irrigation and Drainage, Shahrood University of Technology, Shahrood, Iran

Received 20 June 2016; Accepted 23 February 2017

### ABSTRACT

Irrigation with wastewater can increase the available water supply and present a feasible alternative for increasing resources in water-scarce areas. Despite these benefits, some potential negative environmental effects among which degradation of the hydraulic soil properties and groundwater contamination may arise in association with the use of wastewater. Because of these concerns, a randomized complete block design under unsaturated, steady-state flux was performed with aerobic sand columns treated with synthetic wastewater. Water treatments included four irrigation, and different levels of chemical oxygen demand (COD). A time domain reflectometry (TDR) probe was used to measure water content and electrical conductivity at two depths of 20 and 60 cm from the top of columns. Water samples were taken using Rhizon extractors placed at 25 cm and 65 cm from the top. At each column two tensiometers for measuring hydraulic potentials were placed, at two different depths 20 and 60 cm. Four steady-state flux conditions (1 cm h<sup>-1</sup>) tracer tests were used to obtain transport parameters such as the dispersion coefficient and pore-water velocity by analyzed a transfer-function method. Estimating water and solute transport parameters was simulated by inverse modelling techniques. Statistical analysis shows that transport parameters under the unsaturated conditions were remained fairly constant in all treatments during the experiment time. In contrast, after exploring different possible shapes for a curve the experimental data were fitted in a simple model for evaluating the zero order and first order form of rate equations to evaluate the kinetics. It was found that first order rate expression is the best fit for the synthetic wastewater under different concentrations that gives a best fit shape constant ( $R^2 = 0.9714$ ). Overall, the HYDRUS-1D model successfully simulated the water flow and Pulse-response experiments in the columns. If during primary stages of municipal wastewater treatment, some elements like solids, the toxics or pathogens be removed, which is essential for trickle irrigation, then the municipal wastewater can be similar to our artificial wastewater. The results show that the effluent of our synthetic wastewater without toxic or pathogen elements, was very clear and its quality exceeded the direct discharge standard, poses little risks for groundwater pollution. In addition, the experimental results also show that the removal efficiencies of COD was high, being more than 65% and 95%.

*Keywords:* Irrigation; Synthetic wastewater; Chemical oxygen demand; Solute transport; HYDRUS-1D

### 1. Introduction

Water scarcity, population growth and economic development are among the main problems to be faced by many

societies especially in arid and semi-arid areas. Due to the high evaporation and the lack of rainfall in these areas it is necessary to irrigate the fields to increase the agricultural production [1]. Wastewater irrigation is a widely used practice worldwide, in arid and semiarid regions, to alleviate water shortages in agriculture [1–4]. Uses of municipal wastewater in irrigation can mitigate the utilization

\*Corresponding author.

of natural water resources and enables the diversion of nutrients from water bodies by using soil and plants as natural filters but if mislead, can cause serious environmental and economic harm. Various studies confirm that treated sewage waste water can be useful as an additional water resource for irrigation [5,6]. However, degradation of soil hydraulic properties is one of the expected risks of wastewater reuse. Chemical clogging includes swelling and dispersion of clay particles that are induced by sodium concentrations generally higher than those for the associated fresh water [7,8]. Biological clogging is caused by soil pore size reduction due to bacterial growth and/or accumulation of by-products, in aerobic or anaerobic conditions [9,10]. Severe clogging of the surface soil layer may lead to anoxic soil conditions, reduced infiltration and redistribution of water in the root zone, and diminished effectiveness of the wastewater treatment [11,12]. Transformation of a substance into new compounds through biochemical reactions or the actions of microorganisms in soils is based on processes that control the transport of solutes through the unsaturated zone [13]. The organic compounds in soil undergoes a lot of change. Biodegradation is the transformation of a substance by micro-organisms. Under environmental conditions, biodegradation can be affected by a number of factors, including the presence of oxygen (aerobic/anaerobic conditions) and nutrients, the population size of the required microorganisms, and the micro-organisms' adaptation [14]. The organic compounds that dissolve in groundwater move more slowly than groundwater because of sorption to the soil particles (Suzanne Lesage). The solubility of a compound and its sorption in soil are inversely related: i.e. increased solubility results in less sorption. Pesticide solubility is an important factor in waste disposal. Solubility can indicate the maximum amount of pesticide in solution in any accidentally contaminated water. Compounds with high degrees of solubility are expected to leach into groundwater. Compounds solubility is an important factor in solute transport in soil. Solubility can indicate the maximum amount of compounds in solution in any accidentally contaminated water. Compounds with high degrees of solubility are expected to leach into groundwater. Many sand filters operate under water-saturated conditions. This leads to anaerobic conditions amplified by the waste water's large oxygen demand. As an alternative to sand filters, soil filters have been used for treatment of agricultural wastewaters [15] and as a cost effective alternative to conventional septic tank/soil adsorption systems for domestic wastewater [16].

The purpose of this paper is to present experimental results of solute transport through twelve PVC tube with a 200-mm inside diameter (ID) and a length ( $L_1$ ) of 800 mm soil columns. Tracer experiments with a  $\text{CaCl}_2$  solution were conducted during steady unsaturated water flow into a sandy column homogeneous. Synthetic wastewater was used as the source of nitrogen, carbon and phosphorus for all columns during experiment time. Transport parameters and degradation were studied in laboratory soil columns. Effective average pore-water velocities and dispersion coefficients were estimated by a transfer-function of method to the breakthrough curves observed at regular intervals along the horizontally placed columns. The Hydrus-1D

software package [17] was used in computation of Richards's flow and convection dispersion (CDE) solute transport equations.

## 2. Theory

### 2.1. Transport and degradation of dissolved material in a soil

The simple formulation of the one-dimensional convection-dispersion equation (CDE) under steady-state one-dimensional water flow and with degradation is:

$$R \frac{\partial C}{\partial t} = D \left( \frac{\partial^2 C}{\partial x^2} \right) - V \left( \frac{\partial C}{\partial x} \right) - \mu C \quad (1)$$

with  $C$  ( $\text{M L}^{-3}$ ) the solute concentration,  $D$  ( $\text{L}^2 \text{T}^{-1}$ ) the dispersion coefficient, and  $v$  ( $\text{L T}^{-1}$ ) the average solute velocity estimated as, where  $q$  is the Darcy flux density ( $\text{L T}^{-1}$ ) and  $\Theta_v$  is the effective volumetric water content ( $\text{L}^3 \text{L}^{-3}$ ),  $x$  is distance (L). In general,  $D$ ,  $v$ , and  $\Theta$  are functions of both  $t$  and  $x$ . The constant  $\mu$  ( $\text{T}^{-1}$ ) is the rate constant, and describes first-order degradation. The parameters  $D$  and  $v$  were obtained from fitting the analytical solutions of Eq. [1] to BTCs observed during steady-state flow leaching experiments using a least-squares optimization procedure. Hydrodynamic dispersion  $D$  ( $\text{L}^2 \text{T}^{-1}$ ) incorporates the effect of both mechanical dispersion and molecular diffusion and is often estimated as:

Since molecular diffusion cannot be separated from mechanical dispersion in flowing groundwater, the two are combined into a parameter called hydrodynamic dispersion coefficient,  $D$ :

$$D = \lambda v + D_0 \quad (2)$$

where  $\lambda$  (L) is the mechanical dispersity, and  $D_0$  ( $\text{L}^2 \text{T}^{-1}$ ) the molecular diffusion coefficient. Due to hydrodynamic dispersion, the concentration of a solute will decrease over distance.

## 3. Materials and methods

### 3.1. Measurement of $D$ , $V$ and $m$

The transfer function theory can be used to determine the  $V$  and  $D$  provided the CDE equation is linear [18]. This is realized by firstly applying a constant water flux. During this water flux a pulse of a conservative tracer is injected and the response is measured at a distance from the pulse. The transfer function is fitted on the pulse-response experiment by optimizing the  $D$  and  $V$ .

Having determined  $D$  and  $V$  we can then determine the degradation constant  $\mu$  by measuring concentration at different depth in the profile it is possible to fit the degradation constant.

Under a constant water-flow and top boundary concentration  $C_0$ , the CDE the solution is:

$$C(x) = C_0 \exp \left[ \frac{Vx}{2D} \left( -1 + \sqrt{1 + \frac{4\mu D}{V^2}} \right) \right] \quad (3)$$

Having determined  $V$  and  $D$  by a pulse-response experiment and with a  $C_0$  and one  $C_x$  measured at position  $x$  below the top the degradation constant can be calculated explicitly:

$$\mu = \frac{V^2}{4D} \left[ \left( 1 - \ln \left( \frac{C_x}{C_0} \right) \frac{2D}{Vx} \right) - 1 \right] \quad (4)$$

Alternatively, we can fit a concentration profile with concentrations at several depths in order to determine the degradation constant. So, either we use Eq. (4) directly on one measurement at depth  $x$  or we fit Eq. (3) by a least squares fit on the concentrations at two or more depths.

### 3.2. Experimental setup

Solute and tracer experiment was conducted on twelve soil columns. Fig. 1 shows the experimental setup. A PVC tube with a 200-mm inside diameter (ID) and a length ( $L_{e1}$ ) of 800 mm was placed on a larger PVC tube with ID = 300 mm and ( $L_{e2}$ ) = 1000 mm.

The bottom tube had a water table at 95 cm below the interface between the tubes. In this way the top tube had a bottom boundary condition with a prescribed suction by a hanging water table. A small horizontal hole was drilled in the wall of each bottom column at 50 mm above the closed base in order to allow drainage of water and to maintain the shallow water table. All columns were filled uniformly with sieved natural sand (grain size 0.063–0.125 mm) and flow was directed from the top to the base of the sample to represent vertical 1D flow down through the soil. At the top boundary of the upper soil column steady state water flux consisting of either demineralized water or synthetic wastewater was established with a Mariotte bottle. Water samples were taken using Rhizon extractors placed at 25 cm and 65 cm from the top. A sample is obtained by placing the sampler under vacuum. The vacuum is obtained using a vacuum tube or a syringe. A small suction was applied to all extractors to sample the soil solution periodically. In the top columns water potential was monitored by tensiometers. According to [19], water content and bulk soil electrical conductivity were measured simultaneously

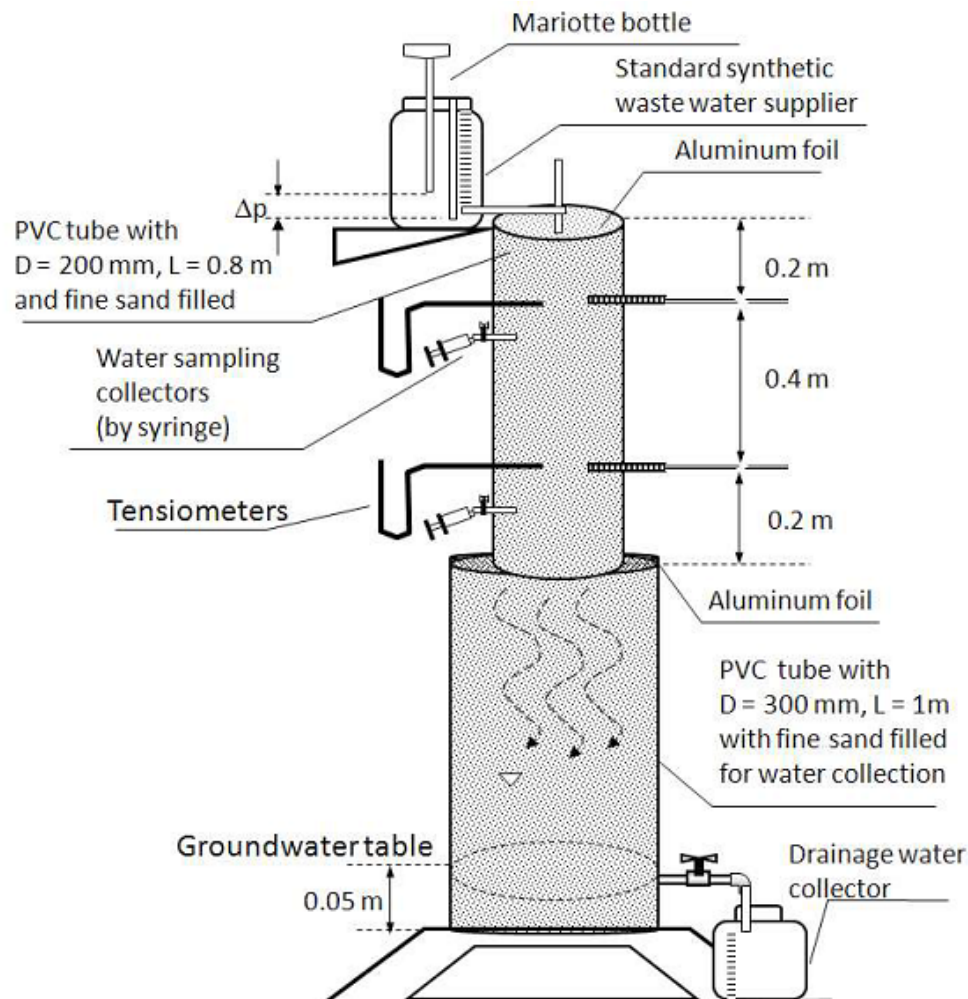


Fig. 1. Sketch of the experimental setup to acquire data on the transport of water and solutes using TDR. All measurements are situated in the top column with 200 mm ID. The bottom column create natural suction for unsaturated flow in the columns.

by Time Domain Reflectometry (TDR). Parallel three-wire TDR probes, 100 mm long, with a wire diameter of 2 mm, and a spacing of 10 mm, were used. TDR probes inserted horizontally at depth of 20 and 60 cm were connected via a SDMX50 multiplexer (Campbell Scientific Ltd., Shepshed, UK) to the Tektronix cable tester 1502B, with RS232 interface. A computer controlled the settings of the TDR and also recorded and analyzed the waveforms using Win TDR software [20]. Measurements of both water content and bulk soil electrical conductivity were taken every 10 min at the beginning and every 30 min after the fourth hour. A rainfall simulator was used to apply the water at a steady rate to each column. At each column two tensiometers for measuring hydraulic potentials were placed, at two different depths (20 and 60 cm from the top). Three times during a day, a cycle of consecutive measurements for the tensiometers was taken at two locations and data were stored. The unsaturated hydraulic conductivity  $k_{unsat}$  ( $L T^{-1}$ ) was estimated by Darcy's law:

$$q = k_{unsat} \frac{\Delta H}{\Delta X} \quad (5)$$

where  $\Delta H$  is the total hydraulic head loss across a length  $L$ . For all tracer tests, the length ( $\Delta X$ ) is 40 cm and corresponded to the distance between to TDR probes. The  $\Delta H$  was determined by the tensiometer-readings and adding the gravitational potential differences. The surface of the soil in the upper columns and annular surface of soil in the lower columns were covered with aluminum foil to prevent evaporation. The steady-state flux condition ( $1 \text{ cm h}^{-1}$ ) was applied.

Alternatively the flux was estimated from a  $\text{CaCl}_2$  tracer test:

$$q = \frac{\Delta x}{t^*} \theta_v \quad (6)$$

where  $t^*$  is the mean travel time of the tracer,  $\Delta x$  the travel distance and  $\theta_v$  the measured volumetric water content.

### 3.3. Synthetic wastewater irrigation

Artificial wastewater was prepared using the following: glucose,  $\text{NH}_4\text{Cl}$ ,  $\text{KH}_2\text{PO}_4$ ,  $\text{K}_2\text{HPO}_4$ ,  $\text{MgSO}_4 \cdot 7\text{H}_2\text{O}$ ,  $\text{NaHCO}_3$  and concentrations of trace salt minerals,  $\text{CaCl}_2$  ( $5 \text{ mg l}^{-1}$ ),  $\text{FeCl}_3 \cdot 6\text{H}_2\text{O}$  ( $0.1 \text{ mg l}^{-1}$ ). The composition of the synthetic wastewater was chosen according to (Houtmeyers 1978), was adjusted according to advise by Rik Deliever (personal communication 2008) and has been used in pilot-water treatment experiments. The concentrations of the major cations chosen for synthetic wastewater are in the range of typical domestic waste water. These values were compared with the standards established for wastewater reuse the Food and Agricultural Organization (FAO) (Pescod 1992) of the United Nations. The chemical composition synthetic wastewater is illustrated in (Table 1).

The experiments were a randomized block design with water at four levels, replicated three times. Treatments were expressed in chemical oxygen demand (COD) concentrations of applied wastewater. Chemical oxygen demand (COD) is a measure of the capacity of water to consume

Table 1

Ingredients of artificial sewage for a COD of  $300 \text{ mg l}^{-1}$  (Houtmeyers 1978). Water having a pH in the range of 7 to 8 adjusted by adding  $\text{NaHCO}_3$  concentration

| Constituent                               | mg l <sup>-1</sup> | Contribution     | Source of     |
|---|--------------------|------------------|---------------|
| Glucose                                   | 225                | 500 C            | Carbon        |
| $\text{NH}_4\text{Cl}$                    | 150                | 40 N and 100 Cl  | N and Cl      |
| $\text{KH}_2\text{PO}_4$                  | 11                 | 2.5 P            | P             |
| $\text{K}_2\text{HPO}_4$                  | 14                 | 2.5 P            | P             |
| $\text{MgSO}_4 \cdot 7\text{H}_2\text{O}$ | 100                | 40 $\text{SO}_4$ | S             |
| $\text{NaHCO}_3$                          | 450                | pH 7.5           | pH adjustment |
| $\text{CaCl}_2$                           | 5                  | Some Ca          | Ca            |
| $\text{FeCl}_3$                           | 0.1                | Some Fe          | Fe            |

oxygen during the decomposition of organic matter and the oxidation of inorganic chemicals such as ammonia and nitrite. A steady unsaturated flow flux conditions ( $1 \text{ cm h}^{-1}$ ) was established in the columns using Mariotte. We donated the treatments as T1 (COD  $300 \text{ mg l}^{-1}$ ), T2 (COD  $200 \text{ mg l}^{-1}$ ), T3 (COD  $100 \text{ mg l}^{-1}$ ) and T4 (COD  $0 \text{ mg l}^{-1}$  as a control). Demineralized water was used to completely and instantaneously for mixing the synthetic wastewater. Demineralized water was used to completely and instantaneously for mixing the synthetic wastewater. Fig. 2 shows the degradation in the Mariotte bottles over time. The degradation appears to be linear, so zero-order degradation can be accepted. Based on these degradation curves it was decided to mix every three days a fresh solution in a tank ( $200 \text{ L}$ ).

### 3.4. Pulse-response experiments

Solute transport parameters were estimated by fitting the convection-dispersion equation to the observed breakthrough curves for each solute at various depths in each column. The data at the upper position was considered as the input and that at the lower position as the response. Before starting the displacement experiment, a constant rate of water flow through the soil columns was established by a Mariotte bottle. Soil surface was then covered by a polyethylene plastic for few days to allow the soil column to reach an equilibrium state. The whole system reaches equilibrium with the applied and drainage water in one week. The equilibrium condition was confirmed from the identical rates of the applied and drainage water for each column and from constant water content and constant suction head by tensiometers and TDR water content readings. Water was spread uniformly over the surface of soil column using a paper filter. Ordinary tap water was used as "tracer-free" but had a small background EC. The salt tracer pulse was applied by changing the water source to the Mariotte bottle from tap water to the Calcium chloride ( $\text{CaCl}_2$ ) solution, which was equivalent to a surface application rate of  $10 \times 10^{-3} \text{ g/cm}^2$ . The pulse duration was 30 min while maintaining the same Mariotte bottle inflow rate before, during and after the pulse application to ensure a constant pore water velocity. The transport of the solute was characterized by monitoring the change in EC at 20 and 60 cm from the top of each column with TDR probe. The measurements of TDR sensors

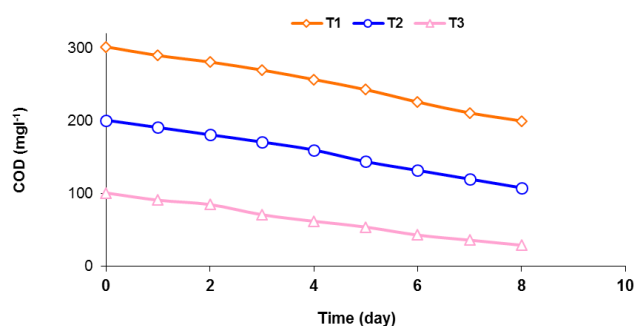


Fig. 2. Degradation of the synthetic wastewater in the Mariotte bottles over time. On the basis of these curves a 3 days interval for mixing fresh solutions was selected. The COD-time relationship seems to be a zero-order decay process.

were performed with a scanning interval of 10 min until the applied water was leached, as confirmed by the reaching a bulk electrical conductivity equal to the background and initial EC before the tracer application.

### 3.5. Analysis of pulse-response data

The EC of the soil solution was calculated from the TDR-measured bulk soil EC via a physically based model by Friedman [23]. According to Chou and Wyseure [24] the background EC was firstly subtracted from the measured EC responses in order to obtain the increase in EC due to the tracer. BTCs constructed from the electrical conductivity (EC) of bulk soil estimated from measurements by time-domain reflectometry (TDR). BTCs constructed from the electrical conductivity (EC) of bulk soil estimated from measurements by time-domain reflectometry (TDR). The solute-transport parameters including pore water velocity and dispersion coefficient were determined through transfer function analysis [18]. The measuring probe of the TDR sensor signal was taken as the input ( $C_{in}$ ) at the top of every column while the response ( $C_r$ ) was taken at the bottom of every column. Eq. (4) was fitted to the measured BTCs normalized EC data. For linear systems with continuous variables, the input and response signals can be related by a transfer-function. In engineering, a transfer function is a mathematical representation for fit or to describe inputs and it is the ratio of the Laplace transform of the output variable to the Laplace transform of the input variable when all initial conditions are zero. The column of soil is assumed to be infinitely long and initially relaxed, that is, the initial concentration of the solute is zero throughout the column. The method was implemented in R software, which is free software environment for statistics and graphics under General Public License (GPL).

### 3.6. Parameters estimation

In this study, numerical model HYDRUS-1D version 4.14 was used as a tool to simulate water and solute movement in the soil columns and transport parameters were then obtained by fitting solutions of the CDE to observed breakthrough data. The HYDRUS-1D program uses the Marquardt-Levenberg optimization algorithm [17] for the

inverse estimation of soil hydraulic and solute transport parameters. The software is based on the least squares method for the parameters optimization and can deal with different water flow and solutes transport boundary conditions [17]. To estimate the hydraulic parameters, Hydrus simulation started using the steady state water flux condition with a low background concentration.

## 4. Results and discussion

### 4.1. Hydraulic properties

Hydraulic properties are important factors controlling the water transport in soils, and hence the leaching of wastewater pollution. The results in this section are presented to have an idea about the water regime in the soil columns. Comparison between simulated and measured water content and relationships between water content versus time are presented in Figs. 3 and 4, respectively. The results show, although there were somewhat deviations in several values, but there was a good agreement between the model and TDR data. At a first glance one could observe that the water content for pure water was somewhat higher. However, looking to the period before COD treatments were started whereby all columns received the same pure water, it is clear that this is a difference in column characteristic. Looking into the changes by subtracting the pre-treatment water content from the actual ones indicates by visual inspection that there was no difference. During experimental period TDR measured average water content was higher at top of soil due to continuous dripping of water and bottom has lower water content due to drainage effect of dune sand. The statistical criteria of quantitative model evaluation were summarized as follows, 0.0221, 0.0071, 0.0110 and  $-0.0055$  ( $\text{cm}^3 \text{cm}^{-3}$ ), and root mean square error values of 0.0912, 0.0295, 0.0479 and 0.0341 ( $\text{cm}^3 \text{cm}^{-3}$ ), for T1, T2, T3 and T4, respectively. For the treatments (T1, T2 and T3), the model systematically overestimates the soil water content by 0.014 to 0.025 ( $\text{cm}^3 \text{cm}^{-3}$ ). Differences between observed and simulated values can result from inappropriate parameter values or lack of the model's ability to simulate processes occurring at a site.

According to the analysis of variance (ANOVA) shown in Table 2 using the changes as compared to the starting values in the same columns confirmed that there was no significant variation in the ( $P < 0.05$ ) between the treatments. Although the water content in soil had some fluctuation during the experiment time, however it was independent of the treatment and or interestingly the fluctuation decreased and reached a balance before the end of experiment period.

Decreased viscosity might be because of temperature effect during a warmer period in the middle of summer. It was checked whether the waste water had a different viscosity as compared to the demineralized water. The water had at a temperature of 20°C a kinematic viscosity of 1.004 centistokes. Our sample with a concentration of 100  $\text{mg l}^{-1}$  and 1500  $\text{mg l}^{-1}$  COD had a kinematic viscosity of 1.0057 and 1.0119 centistokes, respectively. Although the increase in viscosity was measurable in a reliable and reproducible way, the increase was less than 1% as compared to pure water for a COD of 1500  $\text{mg l}^{-1}$ , which is 5 times more than 300  $\text{mg l}^{-1}$ , our highest concentration. So, viscosity effects in function of COD concentration can be excluded. The

effect of concentration on viscosity is smaller than that of temperature. In a similar way there was also no significant difference for changes in unsaturated hydraulic conductivity during the experiment between the treatments (Table 3).

#### 4.2. Solute breakthrough curves

We analysed breakthrough curves of CaCl<sub>2</sub> in 120 experiments to determine the transport parameters in natural sand by the transfer-function method (Table 4). The transport parameters obtained were compared with those determined by the widely used a one-dimensional unsaturated transport model of the Hydrus-1D. First, *D* and *v* were estimated assuming that *R* = 1, then longitudinal dispersion (*λ*) values have been estimated for each of the 120 tracer, through the interpretation of the corresponding breakthrough curve. The pore water velocities determined by the transfer function method using the CaCl<sub>2</sub> pulse-response were in good agreement with the pore water velocities estimated by combining the column cross-sectional area, volumetric flow rates, and water contents. The fluxes estimated from the CaCl<sub>2</sub> mean arrival times and water contents were in good agreement as compared to the imposed fluxes. The measured pore water velocity also varied along the soil column due to non-uniform water content that indicate our soils have preferential flow in their porous medium. Flourey

et al., (1994) mentioned that fine textured soil has the preferential flow, like this condition also occur in unsaturated sandy soils due to textural variations and water repellency. This type of flows may also arise from fluid instability or due to variation of water and solute input at the soil and such flow is unpredictable (Kamara et al., 2001). However we used average water content and assumed constant velocity over the observation length of column. De Smedt and Wierrega (1978) found that despite non-uniform water content distributions, BTCs of solutes moving through

Table 2  
Analysis of variance for water content

| Source             | <i>D<sub>f</sub></i> | Sum of squares | Mean square | F     | Sig.                |
|--------------------|----------------------|----------------|-------------|-------|---------------------|
| Between treatments |                      |                |             |       |                     |
| Treatment          | 3                    | 0.014          | 0.005       | 0.948 | 0.419 <sup>ns</sup> |
| Block              | 11                   | 0.018          | 0.002       | 0.325 | 0.980 <sup>ns</sup> |
| Residual           | 189                  | 0.933          | 0.005       |       |                     |
| Between weeks      |                      |                |             |       |                     |
| Week               | 12                   | 0.063          | 0.005       | 1.072 | 0.386 <sup>ns</sup> |
| Block              | 11                   | 0.014          | 0.001       | 0.264 | 0.991 <sup>ns</sup> |
| Residual           | 180                  | 0.884          | 0.005       |       |                     |

<sup>ns</sup>= Non significant

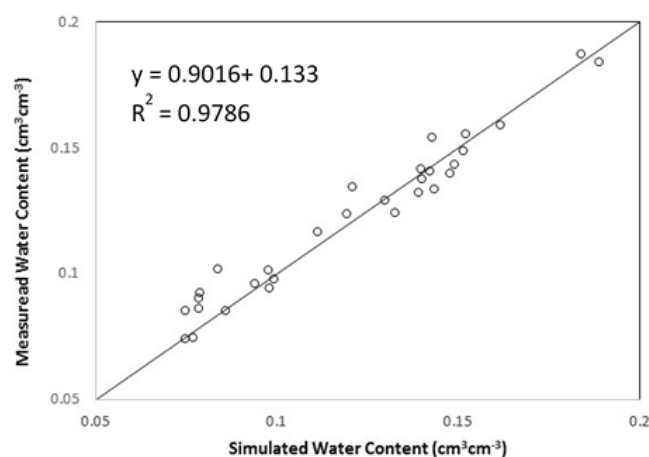


Fig. 3. Comparison of simulated and measured soil water content for the soil columns during experiment time.

Table 3  
Analysis of variance for unsaturated hydraulic conductivity

| Source             | <i>D<sub>f</sub></i> | Sum of squares | Mean square | F     | Sig.                |
|--------------------|----------------------|----------------|-------------|-------|---------------------|
| Between treatments |                      |                |             |       |                     |
| Treatment          | 3                    | 0.839          | 0.280       | 0.341 | 0.796 <sup>ns</sup> |
| Block              | 11                   | 7.202          | 0.655       | 0.799 | 0.641 <sup>ns</sup> |
| Residual           | 189                  | 154.968        | 0.820       |       |                     |
| Between weeks      |                      |                |             |       |                     |
| Week               | 12                   | 13.459         | 1.122       | 1.418 | 0.161 <sup>ns</sup> |
| Block              | 11                   | 7.836          | 0.712       | 0.901 | 0.541 <sup>ns</sup> |
| Residual           | 180                  | 142.348        | 0.791       |       |                     |

<sup>ns</sup>= Non significant

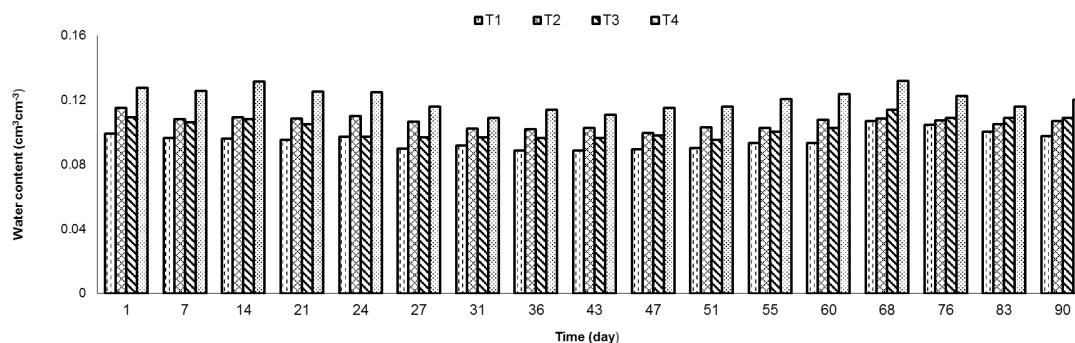


Fig. 4. The relationship between the volumetric water content (*θ*) rate over time for different treatments in soil columns.

unsaturated porous medium under steady state water flux conditions can be predicted using average water content.

The measured and estimated solute breakthrough data for the transport experiment in the all sand columns (Fig. 5) show relatively regular and symmetrical distributions at most measuring points with a good fit. Coefficients of determination  $R^2$  are very high for almost all columns calculations (majority shows from 0.94 to 0.99). The measured breakthrough curves by the displacement experiment and simulated curves with Hydrus-1D are shown in Fig. 4 for different treatments. The correlation between measured and estimated response is poorly correlated in laboratory BTCs data, due to the unavoidable non-uniform spreading solute pulse water steam over the surface of the soil. Mojid et al. [18] mentioned, that the variability of non-uniformity might have caused by variable concentration of solute in water across the cross section of the soil plane and TDR sensors can be detected a cylindrical volume with the diameter approximately 1.4 times of the spacing on the outer sensor (Backer and Lascano, 1989). The diameter of cylindrical volume measured by TDR was approximately 7 cm, while column diameter was 19.2 cm. As a result, about more than half of the column cross-sectional area was not monitored by sensors. However non-uniformity in the horizontal distribution of soil water between the detected and undetected area might have resulted in different BTCs curve in both column. But HYDRUS simulated BTCs curve has higher correlation between measured and response

due to the uniformity of water content. The comparison of the measured relative EC (open circles) and the simulated results from inverse modelling (full line) is given in Fig. 6. Analysis of variance (ANOVA) shows that transport parameters under the unsaturated conditions were remained fairly constant in all treatments during the experiment time (Tables 5 and 6). The observed variances were all attributed to the experimental error. No treatment effect was significant. The variation between the columns was much larger than between the treatments, so effect could be detected. However, these variations in velocity between the columns might be due to some preferential flows of water in the soil columns through regions undetected by the TDR sensor that occurred from non-uniform distribution of soil water in the horizontal plane of the column. Non-homogeneous bulk density of the soils might have caused this variation in hydraulic conductivity and water flow. The results show that the longitudinal dispersivity increased with increasing transport distant. Moreover, the variation of dispersivity respect to the scale of measurement seems to be related to the total porosity of porous media.

#### 4.3. COD degradation

The degradation of synthetic wastewater in the soils may follow either a first-order reaction model or zero-order reaction model. Since it is one of the most important fac-

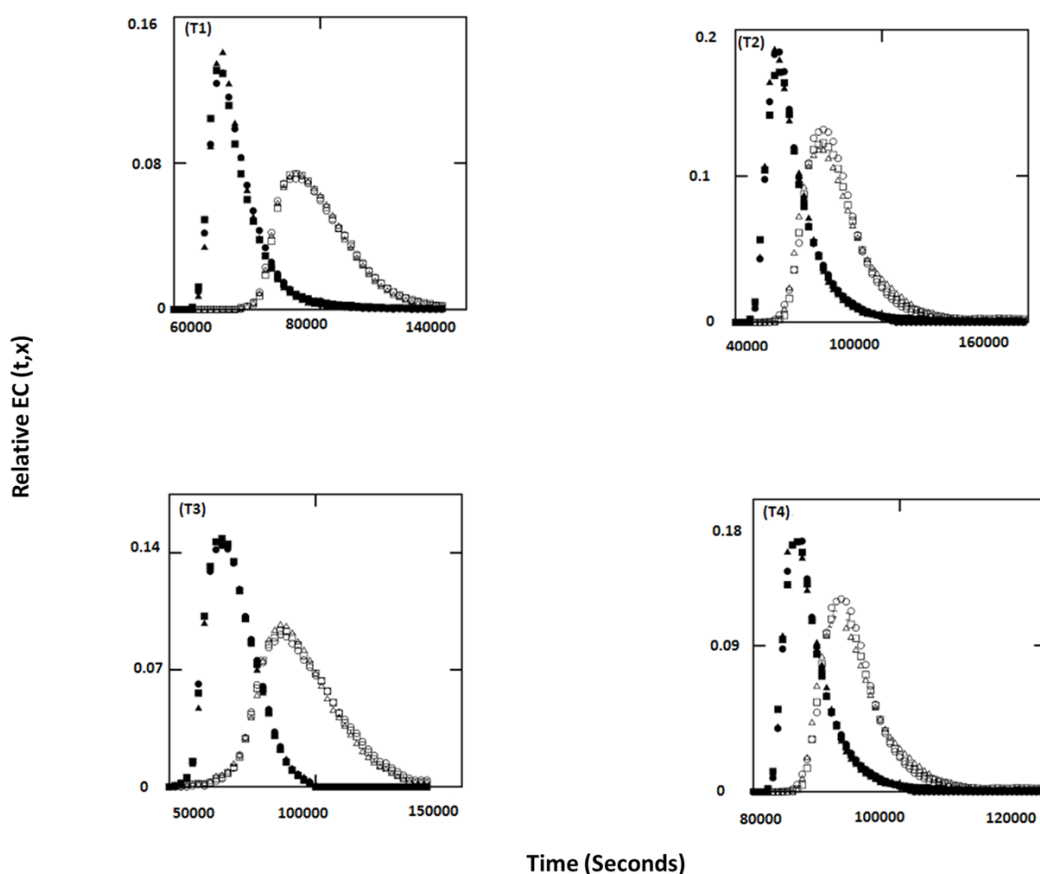


Fig. 5. Example of fitting between the measured and estimated response curves for impulse input of calcium chloride in the flux of  $1 \text{ cm hr}^{-1}$  for all COD-treatments in the soil columns ( $\blacktriangle$ , input 1;  $\bullet$ , input 2;  $\blacksquare$ , input 3;  $\blacktriangledown$ , response 1;  $\circ$ , response 2;  $\square$ , response 3).

Table 4  
Summary of estimated transport parameters from laboratory and HYDRUS simulated BTCs data – Analysis by transfer function method

| Treatments                        |    | $\theta(v)$<br>cm h <sup>-1</sup> | $V$<br>cm <sup>2</sup> h <sup>-1</sup> | $D$<br>cm | $l$<br>– | $R^2$<br>– | RMSE   |
|-----------------------------------|----|-----------------------------------|--|-----------|----------|------------|--------|
| Before treatment                  |    | 0.118                             | 4.27                                   | 0.17      | 0.039    | 0.9088     | 0.2817 |
| During irrigation with wastewater | T1 | 0.136                             | 2.98                                   | 0.18      | 0.060    | 0.9603     | 0.1853 |
|                                   | T2 | 0.127                             | 2.35                                   | 0.50      | 0.212    | 0.9781     | 0.1329 |
|                                   | T3 | 0.117                             | 3.00                                   | 0.73      | 0.243    | 0.9859     | 0.1096 |
|                                   | T4 | 0.134                             | 5.17                                   | 1.76      | 0.340    | 0.9117     | 0.2764 |
| After irrigation with wastewater  | T1 | 0.131                             | 2.00                                   | 2.52      | 1.26     | 0.9819     | 0.1128 |
|                                   | T2 | 0.128                             | 6.77                                   | 1.74      | 0.257    | 0.9466     | 0.2177 |
|                                   | T3 | 0.137                             | 2.72                                   | 0.97      | 0.356    | 0.7724     | 0.3473 |
|                                   | T4 | 0.129                             | 2.75                                   | 0.85      | 0.309    | 0.9013     | 0.2763 |
| Hydrus-1D                         |    | 0.136                             | 6.83                                   | 1.89      | 0.276    | 0.9724     | 0.1569 |

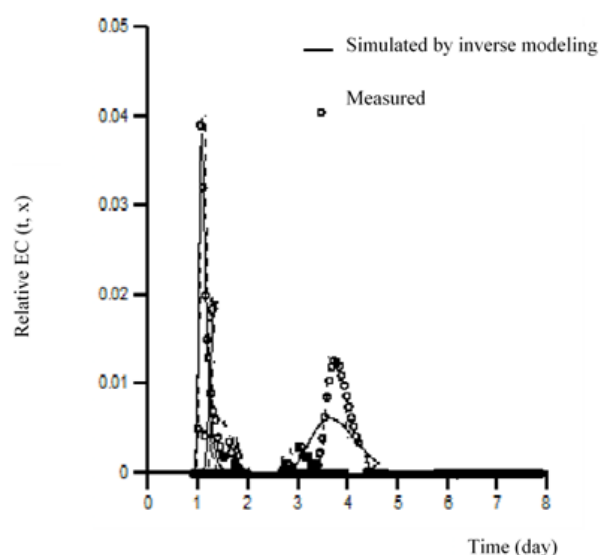


Fig. 6. Comparison of the measured relative EC (open circles) with the simulated results from inverse modelling (full line) ( $r^2 = 0.89$ ) in flux of 1.0 cm hr<sup>-1</sup>.

tors controlling the fate and transport of pollution in soils, the leaching potentials under both types of reaction were evaluated. A simple kinetic model to represent the biodegradation behavior obtained in the laboratory was used to understand the reaction rate. It was revealed that the efficacy of synthetic waste water degradation decreased in the course of time which is (was) shown as decreasing degradation kinetic constant  $\mu$ . Additionally, in all COD treatments, this decrease seems to be the same.

The resulting biodegradation and growth kinetics were best described by the sum kinetics with interaction parameters model. We expected less degradation in the column. Least squares fitting of the degradation constant  $\mu$  in equation 3 were possible for all 200 and 300 concentration and for most 100 mg l<sup>-1</sup>. The direct estimation of  $\mu$  by Eq. (4) on the measured COD at 25 cm depth was possible for all measurements. Comparing the available 2-point fits with direct top

Table 5  
Analysis variance for pore water velocity

| Source             | $D_f$ | Sum of squares | Mean square | F     | Sig.                |
|--------------------|-------|----------------|-------------|-------|---------------------|
| Between treatments |       |                |             |       |                     |
| Treatment          | 3     | 32.090         | 10.697      | 0.935 | 0.425 <sup>ns</sup> |
| Block              | 11    | 80.900         | 7.355       | 0.643 | 0.790 <sup>ns</sup> |
| Residual           | 189   | 2161.430       | 11.436      |       |                     |
| Between weeks      |       |                |             |       |                     |
| Week               | 12    | 188.866        | 15.739      | 1.413 | 0.163 <sup>ns</sup> |
| Block              | 11    | 68.289         | 6.208       | 0.557 | 0.861 <sup>ns</sup> |
| Residual           | 180   | 2004.654       | 11.137      |       |                     |

<sup>ns</sup> = Non significant

fits showed that the direct estimation with concentration at 25 cm depth were in very good agreement. As a result the direct estimations based on the 25 cm deep concentration were used. After exploring different possible shapes for a curve the following equation was able to fit and was selected:

$$\mu(t) = \mu_0 - \mu_d \left( \frac{Kt}{1 + Kt} \right) \quad (7)$$

whereby  $\mu_0$  is the starting value for time 0;  $\mu_d$  the reduction in degradation after a long time  $t$  and  $K$  a shape constant. As shown in Fig. 7 the general fit on all data and the fit on the separate treatments coincide.

For the general fit  $\mu_0$  and  $\mu_d$  was 1.22E-04 s<sup>-1</sup> and 9.19E-05 s<sup>-1</sup>, respectively. Therefore, a final degradation constant around 3E-05 s<sup>-1</sup> (or 2.6 d<sup>-1</sup>) could be expected if the trend continues. The  $K$  fitted on all data was 10.0 while for 300, 200 and 100 COD we found 20.0, 6.3 and 12.0, respectively. The final degradation constant appeared to be the same for all treatments. However one could expect a faster decline (or lower  $K$ ) of the degradation constant for higher concentrations. Especially if there would be some effect of filtering present in an apparent  $\mu$  the decline should be faster with the larger concentration. Filtering effects are unlikely how-



Table 6  
Analysis variance for hydrodynamic dispersion

| Source             | $D_f$ | Sum of squares | Mean square | F     | Sig.                |
|--------------------|-------|----------------|-------------|-------|---------------------|
| Between treatments |       |                |             |       |                     |
| Treatment          | 3     | 93.242         | 31.081      | 1.969 | 0.120 <sup>ns</sup> |
| Block              | 11    | 248.671        | 22.606      | 1.432 | 0.161 <sup>ns</sup> |
| Residual           | 189   | 2983.558       | 15.786      |       |                     |
| Between weeks      |       |                |             |       |                     |
| Week               | 12    | 226.153        | 18.846      | 1.190 | 0.293 <sup>ns</sup> |
| Block              | 11    | 263.034        | 23.912      | 1.510 | 0.131 <sup>ns</sup> |
| Residual           | 180   | 2850.647       | 15.837      |       |                     |

<sup>ns</sup> = Non significant

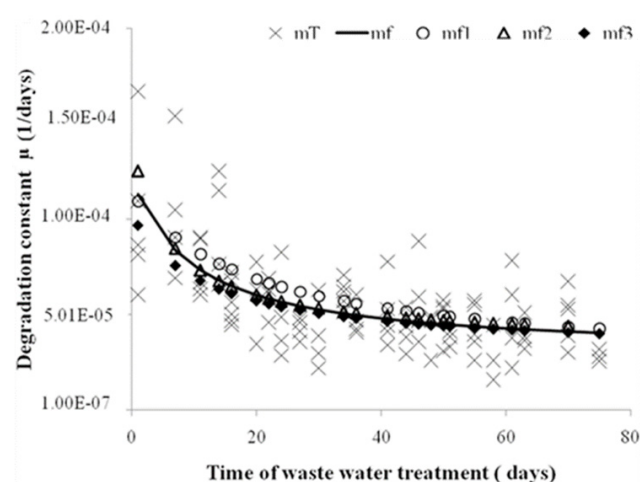


Fig. 7. Degradation constant of the synthetic wastewater in the soil columns over time. The “mT” are the degradation constants  $\mu$  estimated in individual column by Eq. (4) with the concentration at the top 25 cm. The “mf” are the degradation constants  $\mu$  simultaneously fitted on all COD-treatments. The “mf1”, “mf2” and “mf3” are the degradation constants  $\mu$  fitted at the 300, the 200 and 100 mg l<sup>-1</sup> COD, respectively (average for 3 replication).

ever as our synthetic wastewater is composed by highly soluble components without any solids.

The degradation kinetics of synthetic wastewater under different concentration followed first-order kinetics. However with time, the efficiency of the degradation of synthetic wastewater dropped, as observed by the decreased degradation constant. It was expected that the degradation constant would increase as an adapted microbiological community would adapt and become more adjusted to the wastewater as a nutrient. As the synthetic wastewater does not contain any toxic or more difficult to digest constituents it could be that bacteria grow very fast and do not need a lag-time more than a few days. The reduction of the constant could be caused by a built-up of some element in the soil solution. This could be salinity, caused by the tracer, although the salinity always returned quickly to the background level and CaCl<sub>2</sub> should not be

harmful. Other possibility could be some intermediate product or a change in pH.

## 5. Conclusions

Comprehensive understanding of agricultural irrigation with reclaimed wastewater is essential. The present study aimed at performing sand columns system and evaluating the changes of unsaturated flow for wastewater treatment from simulated synthetic wastewater. HURDUS-1D model was used to simulate and inversely estimate the unsaturated soil hydraulic and solute transport parameters with same laboratory model with lower boundary as free drainage and seepage face. On the basis of the following conclusions can be drawn. Research results showed that under unsaturated conditions of synthetic wastewater containing different concentrations no significant differences were observed between the treatments. A first-order kinetic model was a good representation of biodegradation of synthetic wastewater in the soil columns. However, the degradation constant decreased with time and this decrease was independent of the concentration of the wastewater. In spite of the considerable input data demands, HYDRUS-1D successfully simulated the water regime, as well as the effects of different irrigation waters on the soil hydraulic parameters. The model evaluation results provided some guidance for the design of future experiments.

## Acknowledgements

The authors are grateful to the Department of Earth and Environmental Sciences of KULeuven, Belgium, for using their lab facilities to perform the experiments.

## References

- [1] A. Erfani, Environmental aspects use of treated municipal wastewater in irrigation. Published and presented in Iranian National Committee on Irrigation and Drainage (IRNCID), 1996.
- [2] C. Scott, N. Faruqui, L. Raschid-Sally, Wastewater Use in Irrigated Agriculture: Management Challenges in Developing Countries. CABI Publishing, International Water Management Institute, 2004.
- [3] F.P. Huibers, B.B. Van Lier, From unplanned to planned agricultural use: making an asset out of wastewater. The Netherlands: Springer, 2009.
- [4] M. Qadir, D. Wichelns, L. Raschid-Sally, P. McCornick, P. Drechsel, A. Bahri, P. Minhas, The challenges of wastewater irrigation in developing countries, *Agri. Water Manage.*, 97 (2010) 561–568.
- [5] A.M. Palese, V. Pasquale, G. Celano, G. Figliuolo, S. Masi, C. Xiloyannis, Irrigation of olive groves in Southern Italy with treated municipal wastewater: effects on microbiological quality of soil and fruits, *Agric. Ecosyst. Environ.*, 129 (2009) 43–51.
- [6] N. Mehrdadi, H.G. Joshi, T. Nasrabadi, H. Hoveidi, Application of solar energy for drying of sludge from pharmaceutical industrial waste water and probable reuse, *Int. J. Environ. Res.*, 1 (2007) 42–48.
- [7] J. Tarchitzky, Y. Golobati, R. Keren, Y. Chen, Wastewater effects on montmorillonite suspensions and hydraulic properties of sandy soils, *SoilSci. Soc. Am. J.*, 63 (1999) 554–560.

- [8] J.C. Menneer, C.D.A. McLay, B. Lee, Effects of sodium-contaminated wastewater on soil permeability of two New Zealand soils, *Aust. J. Soil Res.*, 39 (2001) 877–891.
- [9] R.C. Rice, Soil clogging during infiltration of secondary effluent, *J. Water Pollut. Control Fed.*, 46 (1974) 708–716.
- [10] P. Vandevivere, P. Baveye, Relationship between transport of bacteria and their clogging efficiency in sand columns, *Appl. Environ. Microbiol.*, 58 (1992) 2523–2530.
- [11] R.J. Otis, Soil Clogging: Mechanisms and Control. In: *On-Site Wastewater Treatment. Proceedings of the 4th National Symposium on Individual and Small Community Sewage Systems*. ASAE, St. Joseph, MI, 1985, pp 238–250.
- [12] R.L. Siegrist, Soil clogging during subsurface wastewater infiltration as affected by effluent composition and loading rate, *J. Environ. Qual.*, 16 (1987) 181–187.
- [13] C.C. Lee, *Environmental Engineering Dictionary*, 4th ed., Lanham, MD: Scarecrow Press 2005.
- [14] C.L. van Leeuwen, T.G. Vermeire (eds.), *Risk Assessment of Chemicals: An Introduction*, 1–36. (2007) Springer.
- [15] J. Martinez, Solepur: a soil treatment process for pig slurry with subsequent denitrification of drainage water, *J. Agric. Eng. Res.*, 66 (1997) 51–62.
- [16] L.G. Rich, Low-tech systems for high levels of BOD5 and ammonia removal. *Public Works-New Jersey* 127 (1996) 41–42.
- [17] J. Šimůnek, M. Šejna, H. Saito, M. Sakai, M.Y. van Genuchten, the Hydrus-1D software package for simulating the movement of water, heat, and multiple solutes in variably saturated media. Version 4.08. HYDRUS Software Series 3. Department of Environmental Sciences. University of California, Riverside, USA, (2009), pp. 330.
- [18] M.A. Mojid, D.A. Rose, G.C.L. Wyseure, A transfer-function method for analysing breakthrough data in the time domain of the transport process, *Eur. J. Soil Sci.*, 55 (2004) 699–711.
- [19] G.C.L. Wyseure, M.A. Mojid, M.A. Malik, Measurement of volumetric water content by TDR in saline soils, *Eur. J. Soil Sci.*, 48 (1997) 347–354.
- [20] D. Or, S.B. Jones, J.R. Van Shaar, S. Humphries, L. Koberstein, WinTDR, Users guide, Version 6.1. Utah State University/ Soil Physics group, Utah, USA. 2004, Retrieved from: <http://soil-physics.usu.edu/wintdr/index.htm>
- [21] J. Houtmeyers, 1978 Relations between substrate feeding pattern and development of filamentous bacteria in activated sludge processes. *Agricultura* 26 (1978) 1. Faculteitlandbouwwetenschappen. K.U.Leuven, Leuven.
- [22] M.B. Pescod, *Wastewater treatment and use in agriculture*. FAO Irrigation and Drainage Paper 47 Rome, 1992.
- [23] S.P. Friedman, Soil properties influencing apparent electrical conductivity: a review, *Comput. Electron. Agric.*, 46 (2005) 45–70.
- [24] P.Y. Chou, G. Wyseure, Hydrodynamic dispersion characteristics of lateral inflow into a river tested by a laboratory model. *Hydrol. Earth Syst. Sci.*, 13 (2009) 217–228.
- [25] D.W. Marquardt, An algorithm for least-squares estimation of nonlinear parameters, *J. Soc. Ind. Appl. Math.*, 11 (1963) 431–441.